Oxygen deficiency in TiO_2: Similarities and differences between the Ti self-interstitial and the O vacancy in bulk rutile and anatase

Peter Deák,* Bálint Aradi, and Thomas Frauenheim
Bremen Center for Computational Materials Sci., University of Bremen, PoB 330440, D-28334 Bremen, Germany
(Received 18 April 2015; revised manuscript received 15 May 2015; published 13 July 2015)

TiO_2 is an oxygen-deficient, intrinsically n-type material, but it is often debated whether the electrons are donated by oxygen vacancies (V_O) or titanium interstitials (Ti_i). Investigating this issue is complicated by the fact that rutile can self-trap electrons in intrinsic small polaron states, while bulk anatase cannot. The screened hybrid functional HSE06 was proven to account for this phenomenon and has provided quantitatively correct results for V_O in our earlier study. Here, we use it for Ti_i in both rutile and anatase, allowing full spin and symmetry freedom, to shed light on the similarities and differences to V_O. We find that these two defects give rise to very similar fingerprints in electron paramagnetic resonance, infrared absorption, or photoelectron spectra. In weakly reduced rutile, the ground state of both defects is (2+), with two electrons in polaronic traps, bound loosely to the defect. Most of the time, only these latter states (crudely resembling a hydrogenic series, with increasing distance from the defect) are likely to be detected. In anatase, both V_O and Ti_i can be expected to be ionized at room temperature (singly and doubly, respectively), and the next vertical ionization energy is similar in the two defects—and very close to the ionization energy of the bound polarons in rutile. Most signals in paramagnetic resonance experiments on rutile must also be related to the polaron states, and, in general, very special conditions have to be fulfilled to detect electrons localized to V_O or Ti_i itself. We show that, in thermal equilibrium, the dominant defect in intrinsic samples is V_O, and Ti_i can be the majority defect only in strongly reduced anatase, or in case of p-type doping.

DOI: 10.1103/PhysRevB.92.045204 PACS number(s): 71.55.Ht, 71.38.−k, 71.35.Aa

I. INTRODUCTION

TiO_2 is a prototype photocatalyst but has a broad range of other applications as well. At the same time, it is a very interesting material to study the interplay of self-doping, due to oxygen deficiency and carrier self-trapping, because of small polaron states [1]. Bulk TiO_2 has the peculiarity that in its rutile form, only electron-polarons can form, turning a lattice Ti(4+) atom into Ti(3+) [2], while in anatase, only holes get trapped, turning a lattice O(2−) atom into O(1−). This theoretically predicted asymmetry between the two polymorphs [3] has recently been confirmed experimentally [4,5]. (Note, however, that small electron polarons may form at some anatase surfaces [6] but may not on some rutile ones [7].) TiO_2 is intrinsically n-type, but the particular defect, responsible for the donor levels, is under debate [8,9]. Earlier, the n-type conductivity was attributed solely to Ti interstitials (Ti_i) in the entire range of substoichiometry [10], while more recently it was argued that, except for very strongly reduced samples, the oxygen vacancy (V_O) dominates [11]. In this paper, we will show by high level calculations that the latter is indeed the case for intrinsic samples but not for p-doped ones. The experimental distinction of these two defects remains difficult though. In this paper, we concentrate on Ti_i but compare its properties with our earlier results on V_O [12]. We will show, that the relatively easily obtainable experimental fingerprints are very similar. In rutile, small intrinsic electron-polaron states capture the electrons donated by Ti_i or V_O, while both defects give rise to shallow states in anatase. The calculations, however, show also important differences, which could guide further experiments.

The theoretical description of doping in wide band gap materials and of self-trapping by small polaron states has become possible only recently, with corrections for the lack of derivative discontinuity and for the electron self-interaction in standard functionals of density functional theory (DFT), by using either Hubbard U terms [13] or hybrid functionals [14]. With the lack of such corrections, the conduction band (CB) masks the true defect states due to the underestimated band gap and, because of the tendency for delocalization, polaronic states are missed altogether. For an accurate description of defects, the band gap should be reproduced, and the total energy should be a linear function of the fractional occupation numbers. While a $+U$ correction, determined from first principles, does not reproduce the gap, elaborate multi-U schemes, designed to fix both deficiencies of standard DFT, have limited predictive power. Probably the best low-cost solution is to apply empirical nonlocal potentials to fix the gap and enforce the generalized Koopmans's theorem (i.e., the linearity of the total energy with fractional occupation numbers) by a special, nonempirical polaron correction [13]. A more costly but also more accurate alternative is the use of hybrid functionals. The admixture of a nonlocal exchange reintroduces derivative discontinuity and the tendency of Hartree-Fock (i.e., HF-type) exchange for overlocalization might compensate the opposite trend of local/semilocal exchange functionals [15]. With a well-chosen mixing ratio and with appropriate screening, both the linearity and the reproduction of the gap can be achieved [16,17]. The HSE screened hybrid functional uses a 25% admixture of HF exchange and a simple, one-parameter error-function approach for screening it [18]. The screening parameter has been chosen by fitting the band gap of a wide range of semiconductors [19]. Numerical tests [20], as well as theoretical considerations [21], support the use

*Corresponding author: deak@bccms.uni-bremen.de

of 25% HF exchange in materials with medium screening, and, in our experience, this is indeed the one needed to achieve the linearity in most cases, including various defects in TiO_2 [3,12]. Luckily, the standard parameters of HSE, also reproduce the one-particle band gap of TiO_2 well [22]. In contrast, hybrids without screening overestimate both the band gap of TiO_2 and the localization of defect states in it. This seems to be true even for B3LYP (the three-parameter Becke-Lee-Yang-Parr hybrid functional [23]), despite of using only 20% HF-exchange, because small electron-polarons were predicted to exist also in bulk anatase by this functional [24]. Using the standard screening parameter of HSE, but diminishing the mixing ratio [25–27], also leads to deviation from linearity [3]. Apparently, the standard parametrization, HSE06 [19], seems to be a well-balanced approximation for TiO_2, so we apply it in the present paper as well. We note, however, that the simple screening scheme of HSE does not necessarily work in all materials (i.e., there is no guarantee that linearity and the correct band gap can always be achieved by tuning the two parameters of the method) and, e.g., the screened exchange method appears to be more general. As we will show, however, these two methods provide nearly identical results in TiO_2. Ti_i has been investigated recently in numerous $+U$ and hybrid functional studies [27–33], which have revealed important characteristics but resulted also in many differences among themselves regarding the equilibrium charge state, charge transition levels, and the symmetry of this defect. Our recent HSE06 study on V_O was able to provide a qualitatively and quantitatively correct reproduction of the complex experimental situation [12], so it makes sense to calculate the properties of Ti_i on an equal footing. This is reported here, comparing the properties of Ti_i with those of V_O in both rutile and anatase.

II. METHODS

HSE06 calculations have been carried out with Vienna *Ab initio* Simulation Package (VASP) 5.3.3, using the projector augmented wave method [34] and excluding the Ti3p states from the core. A 420 (840) eV cutoff was applied for the expansion of the wave functions (charge density). Results of the bulk calculations can be found in Refs. [3,22]. The lattice constants obtained there are used in this paper, too: $a = 4.567$ Å; $c = 2.944$ Å for rutile, and $a = 3.755$; $c = 9.561$ Å for anatase. The HSE06 band gaps are 3.37 eV in rutile and 3.58 eV in anatase. (N.B.: Low temperature optical experiments yield 3.04 eV for rutile [35] and 3.42 eV for anatase [36], while combined photoelectron and inverse photoelectron spectroscopy gives 3.3 ± 0.5 eV for rutile [37,38]. The latter is relevant for the one-particle band gap calculated in HSE06. GW calculations result in values between 3.34–3.73 eV for rutile and 3.56–4.05 for anatase [39–41], so the HSE06 results match the GW ones well. The discrepancy between the optical and the photoelectron gap is due to strong electron-phonon coupling. For a more detailed discussion, see Ref. [40].)

Defect calculations were carried out in a $2\sqrt{2} \times 2\sqrt{2} \times 4$ (192 atom) supercell in rutile and in a $2\sqrt{2} \times 2\sqrt{2} \times 1$ (96 atom) supercell in anatase, using the Γ approximation. (The dispersion of localized defect (LD) levels was checked in the [1/4,1/4,1/4] point [42] and was found to be insignificant.) The effect of higher defect concentration was checked in a $2 \times 2 \times 3$ (72 atom) supercell of rutile, with a 2^3 Monkhorst–Pack (MP) sampling [43]. Note that the applied supercells are as close to cubic as possible, which is required for the Lany-Zunger method of charge correction (for charged defects, both the total energy and the Kohn-Sham level of LD states were corrected) [44–46] and for an unbiased account of relaxation effects (for which a force criterion of 0.02 eV/Å was applied). The Γ approximation also requires a symmetric multiple of the primitive cell [47]. The dielectric constants for the charge correction were taken from the HSE06 calculations of Ref. [48]. Energies have been aligned based on the average electrostatic potentials far from the defect [44].

III. RESULTS IN RUTILE

It is generally agreed that the intrinsic donors of TiO_2 are due to oxygen deficiency. While TiO_2 samples are termed either "reduced" or "oxidized," it is important to know that even the latter are mostly oxygen deficient: after annealing at 1000 °C in oxygen, the stoichiometry is still $TiO_{1.995}$, corresponding to a concentration of $\sim 3 \cdot 10^{20}$ cm^{-3} of V_O and/or Ti_i [49,50]. First, we briefly recapitulate our results on V_O [12]. In contrast to anatase, pristine bulk rutile is capable of trapping mobile electrons in small polaron states at lattice Ti-sites. Such a free polaron (FP) has a (vertical) binding energy of 0.5 eV with respect to an electron in the CB. The thermal energy necessary to release the self-trapped electron was calculated to be less than 0.1 eV and measured to be 0.024 eV [51]. We have shown that the behavior of V_O in rutile is concentration dependent. In reduced samples (with a V_O concentration of about 2% or higher), the two excess electrons (left in the crystal after removing a neutral oxygen atom) are confined to two Ti neighbors of the vacancy. The ground state is an antiferromagnetic singlet, but a triplet state is almost degenerate with that. The ionization of these states gives rise to the electronic transitions observed in infrared (IR) spectroscopy [52]. The second ionization energy is 1.8 eV (with respect to the CB edge). For smaller V_O concentrations (below ~1%), the excess electrons go into two independent, small polaron states, somewhere in the neighborhood of the vacancy [Fig. 1(a)]. Due to the attractive field of V_O^{2+}, the ionization energies of such bound polarons (BP) are higher than that of the FP, 1.0 eV (first) and 1.4 eV (second), in agreement with photoconductivity and thermoluminescence measurements [53,54]. In "oxidized" (weakly reduced) rutile, V_O is, therefore, in a $V_O^{2+} + 2e^-$ state, and only the small polarons can be observed. However, illumination at very low temperature can replenish the vacancy level from the valence band (VB), and the triplet state can then be observed in electron paramagnetic resonance (EPR) [55,56].

Similar to the case of V_O, we find that in the 192 atom supercell (representing weakly reduced crystals), Ti_i is also losing two electrons to small polaron states in the neighborhood of Ti_i^{2+} [Fig. 1(b)]. As a consequence, the first two vertical ionization energies are nearly identical for V_O and Ti_i. Table I summarizes the calculated ionization energies, i.e., the vertical infrared transitions from intrinsic donor states to the CB edge. (Using the calculated 0 K band gaps of 3.4 eV in rutile and 3.6 eV in anatase, these values can be

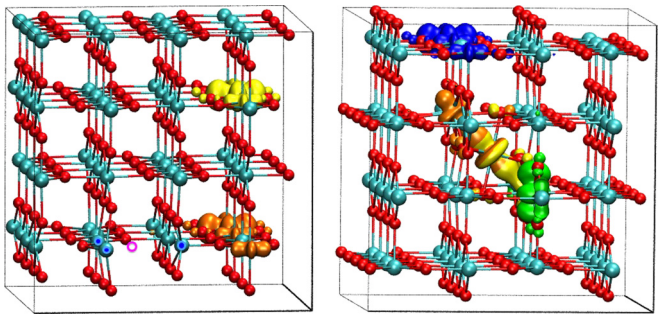

FIG. 1. (Color online) The ground state of V_O (a) and Ti_i (b) in "oxidized" (weakly reduced) rutile. Ti atoms are shown by cyan and oxygen atoms by red spheres. The position of the vacancy and its 3 Ti-neighbors are marked by circles. The lobes depict localized states (orange and green: spin up; yellow and blue: spin down). Black lines mark the periodic simulation cell. V_O looses both of its electrons to polaron traps, i.e., it is in a $(V_O^{2+} + 2e^-)$ state. Ti_i retains two electrons (each shared with one lattice Ti neighbor) and produces two polaronic states, $(Ti_i^{2+}+2e^-)$. The location of the polarons is expected to be random at room temperature.

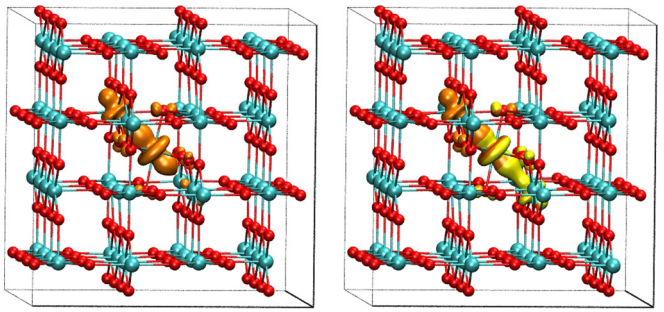

FIG. 2. (Color online) The Ti_i-related spin states of rutile in the (a) (3+) and (b) (2+) charge states of the defect. Color coding is identical with Fig. 1.

converted into peak positions with respect to the VB edge in photoelectron spectroscopy.) We believe that the defect-related state, revealed in valence band photoemission spectra with an energy about 1 eV from the CB edge at room temperature [57–59], is the fingerprint of polarons bound either to V_O or Ti_i.

An important difference between V_O and Ti_i, though, is that in the latter, the number of electrons localized to the defect does not change in the 72 atom supercell either, i.e., Ti_i cannot retain more than two electrons up to a concentration of $\sim 4\%$. This result on Ti_i^0 is in agreement with that of Ref. [31]. We note that constraining the symmetry (to that of Ti_i at the pseudo-octahedral site) does not allow the free formation of independent polaronic states, and this probably explains the deviation from the findings of Refs. [29,33], which predict a symmetric state localized to the first neighbor cation shell.

We would like to emphasize that Ti_i can bind two LD electrons (not only one [32]) in a singlet (antiferromagnetic) configuration. For clarity, the one-electron states of Ti^{3+} and Ti^{2+} are shown in Fig. 2: one electron is shared by Ti_i and one nearest neighbor lattice Ti atom. Prescribing a triplet state sends the second electron of Ti^{2+} off into a small polaron state, too, as in Ref. [32]. From this also follows that, in contrast to V_O, no triplet EPR signal, related to electrons localized on Ti_i, can be expected. If at all, Ti_i should exhibit only an $S = 1/2$ signal related to Ti_i^{3+}. We note that while the ground state is depicted in Fig. 2(a) for this system, a symmetric orbital [the electron shared by Ti_i and both nearest Ti neighbors, in a state that corresponds roughly the sum of the two states shown in Fig. 2(b)] is only 5 meV higher in energy. We expect that at room temperature such a symmetric state will be seen due to motional averaging. We note that the localized electron of Ti^{3+} can also be excited into small polaron states, with discrete energies depending on the distance of the trapping site. The first three excitation energies, 0.13, 0.16, and 0.19 eV resemble closely the series of IR absorption bands at 0.11, 0.15, and 0.17 eV, observed in rutile samples at room temperature [60]. (We note that similar excitation energies can also be expected in the presence of V_O in weakly reduced rutile.) Room temperature IR usually detects vertical transitions, but due to the strong electron-phonon coupling, the Huang-Rhys factor in TiO_2 is high [61], so it is quite possible that the zero-phonon lines of these adiabatic transitions were actually observed. Recently, similar IR transitions have also been observed in ZnO and interpreted in terms of intermediate hole polarons [62]. Large electron polarons were experimentally shown to exist also in anatase TiO_2 [63]. Therefore, we have applied the theoretical formalism used in Ref. [62] for rutile but

TABLE I. Vertical ionization energies (w.r. to the CB, in eV) of intrinsic donor levels in TiO_2. Vacancy results are given for both the high and low concentration (cc) case. The total charge in the system is given in parentheses. The error of these data is estimated, from the level of satisfying the generalized Koopmans' theorem, [13] to be about 0.1 eV.

			Rutile				Anatase
Nature of state	None	V_O^0 (high cc)	$V_O^{2+} + 2e^-$ (low cc)	$Ti_i^{2+}+2e^-$	Nature of state	V_O^0	$Ti_i^{2+}+2e^-$
—	—	—	—	—	EMT	—	0.3(0)
—	—	—	—	—	EMT	—	0.3(1+)
FP	0.5(1–)	—	—	—	LD	0.5(0)	—
LD	—	0.8(0)	—	—	—	—	—
BP	—	—	1.1(0)	1.0(0)	—	—	—
BP	—	—	1.4(1+)	1.4(1+)	LD	1.3(1+)	1.2(2+)
LD	—	1.8(1+)	—	—	—	—	—
LD	—	—	—	2.1(2+)	LD	—	2.1(3+)
LD	—	—	—	2.6(3+)	—	—	—

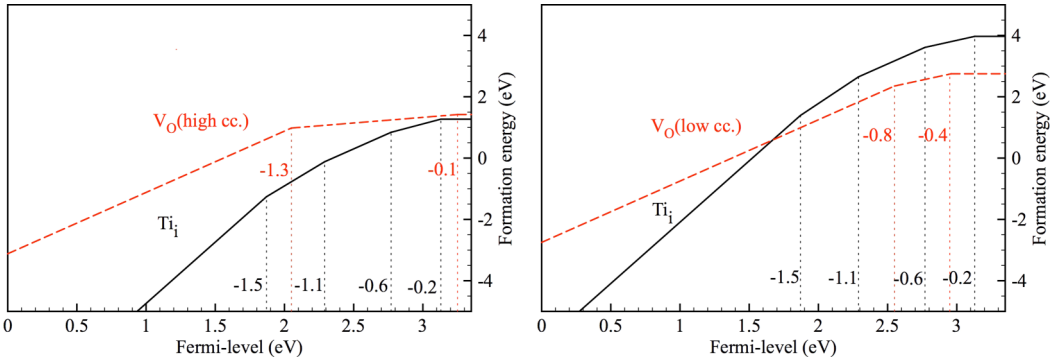

FIG. 3. (Color online) Formation energies of V_O (dashed red lines) and Ti_i (solid black lines) as a function of the Fermi-level position, for extreme oxygen-poor (a) and stoichiometric conditions (b) in rutile. The dotted vertical lines mark the positions of the consecutive charge transitions levels, and the numbers left of these lines give their position with respect to the CB-edge. The error in these data originates mainly from the approximate nature of the charge correction and is estimated to be about 0.1 eV.

could not reproduce the series of IR transitions observed there [60] with large electron or hole polarons. This strengthens the claim that the observed absorption bands may be related to the hopping of small BP between neighbor shells around the center of the binding potential.

The possibility to observe the various charge states of Ti_i, of course, depends on their stability. Figure 3 shows the adiabatic (thermal) charge transition levels of V_O and Ti_i in rutile, for extreme oxygen poor and for stoichiometric conditions, i.e., for the limiting cases of oxygen deficiency. (N.B.: the extreme oxygen poor condition corresponds to the limit of Ti_2O_3 formation.) In agreement with Ref. [33], our calculated formation energies support the arguments of Ref. [11] about V_O being the dominating defect in intrinsic rutile, except for very strongly reduced samples. The presence of acceptors will, however, push the Fermi level towards the VBM, increasing the concentration of Ti_i faster than that of V_O. The latter fact is quite important from the view-point of band gap engineering in rutile with nitrogen- (p-type) doping for visible-light photocatalysis [64–66].

In contrast to Ref. [33], we find all charge states to be stable in some window of Fermi-level positions. Our value for the first ionization energy of V_O in weakly reduced ("oxidized") rutile, 0.4 eV, is supported by experiments [54,67]. We note that the first two ($0/+$ and $+/2+$) charge transition levels of V_O in weakly reduced rutile and of Ti_i in any case, are related to polaron states bound by but not localized to the defect (see Fig. 1). Unlike the vertical ones, however, these adiabatic (thermal) ionization energies are different for V_O and Ti_i. Somewhat surprisingly, the first adiabatic ionization energy of V_O in strongly reduced rutile (i.e., from a state localized to a vacancy neighbor) is less than that of the polaron bound to Ti_i. According to our results, the higher charge states, with electron states localized to Ti_i are also stable and have likely been observed in photoluminescence experiments on nanoribbons [68].

IV. RESULTS IN ANATASE

Anatase, with no polaronic electron traps, is more prosaic also in terms of the intrinsic donor levels. Table I provides the nature of the donor states and their vertical ionization energies in anatase, too. In anatase, V_0 and Ti_i are qualitatively different. As shown in Fig. 4(a), V_O retains its electrons on LD states (with a relatively shallow first ionization energy). The ground state is a neutral, antiferromagnetic singlet, and the two electrons are shared by the three Ti neighbors of the vacancy [12]. In contrast, Ti_i gives rise to two effective-masslike (EMT) states, even shallower than the localized states of V_O. The electrons in these EMT states are essentially delocalized. Ti_i retains two electrons in an antiferromagnetic singlet configuration [(Fig. 4(b)], quite similar to that of V_O^0. In end effect, one could say that Ti_i can only exist as ($Ti_i^{2+}+2e^-$) in both rutile and anatase, weakly binding two electrons in BP or EMT states, respectively.

Taking into account the inaccuracy of the calculations, the possible vertical ionization energies (with respect to the CB edge, as shown in Table I) of V_O and Ti_i seem to be "bunched" also in anatase: the first ionization energy of V_O is close to that of the EMT states of Ti_i and so is the second ionization energy of V_O to the third of Ti_i. Considering that—in agreement with experiment [69]—the first adiabatic ionization energy of both V_O and Ti_i are shallow [70] in anatase (much shallower than in rutile, cf. Figs. 3 and 5), it is expected that, in intrinsic anatase at room temperature, V_O is practically always singly and Ti_i always doubly ionized. Therefore, the observed characteristic photoelectron peaks must be related to these states, and they have almost the same position with respect to the CB edge, actually very close to those of the BP peaks of rutile. When surface related BP-s at nearly the same

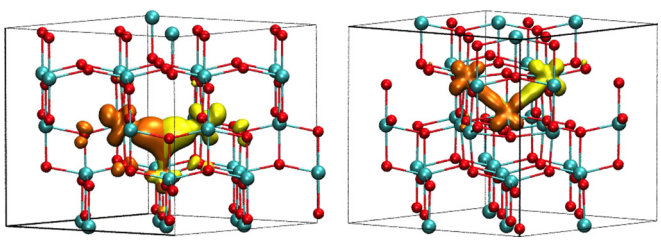

FIG. 4. (Color online) The localized states of neutral V_O (a) and Ti_i (b) in anatase. In case of Ti_i, two other electrons are in delocalized EMT states (not shown). Color coding is the same as in Fig. 1. The defects are in the middle of the cells.

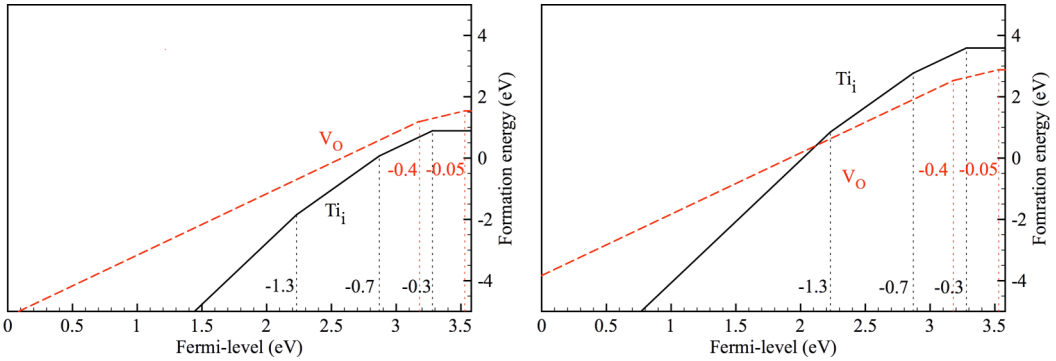

FIG. 5. (Color online) Formation energies of V_O (dashed red lines) and Ti_i (solid black lines) as a function of the Fermi-level position, for extreme oxygen-poor (a) and stoichiometric conditions (b) in anatase. The dotted vertical lines mark the positions of the consecutive charge transitions levels, and the numbers left of these lines give their position with respect to the CB-edge. N.B.: Considering the accuracy of these calculations, the value of 0.05 eV is just an indication for an ionization energy between 0.1 and 0.0 eV.

energy are also considered [6,71], it seems that the polymorph- and orientation-independent photoelectron peak, at about 1 eV below the CB edge [57–59], deserves closer examination [72].

Finally, we note that based on Fig. 5 (and in agreement with Ref. [28]), we find V_O to be the dominant defect in weakly reduced anatase as well, for almost all Fermi-level positions. However, Ti_i seems to play a more significant role in strongly reduced anatase than in rutile. This result is confirmed by recent experiments that also point out the importance of Ti_i in the band gap engineering of anatase for visible light photocatalysis [68]. We find that the charge states Ti_i^{2+} and Ti_i^{3+}, can be stabilized at appropriate Fermi-level positions and should be observable in *p*-type samples. We also note that, very recently, methods have been developed to synthetize oxygen rich TiO_2, showing intrinsic *p*-type doping [73]. The latter is attributed to Ti vacancies, which are being assumed to be responsible for the observed intrinsic room temperature ferromagnetism [74]. Defect engineering to exploit these possibilities, will certainly be influenced by the counterdoping effect of the intrinsic multiple-donor Ti_i.

V. SUMMARY

Using the screened hybrid functional HSE06, we have investigated the cation interstitial Ti_i in bulk rutile and anatase and compared its properties to our earlier findings on the anion vacancy V_O. Since HSE06 reproduces the one-particle gap and satisfies the generalized Koopmans' theorem for LD levels within 0.1 eV, it can provide reliable vertical electronic and adiabatic charge transition levels, as was proven in the case of V_O by comparing with available experimental data [12]. For Ti_i, we find that all charge states between Ti_i^{4+} and Ti_i° can be stable, but a maximum of only two electrons are actually localized to the interstitial. Further, electrons go onto shallow EMT orbitals in anatase or into small polaron states bound by the ionized interstitial in rutile. Therefore, in weakly reduced rutile, V_O and Ti_i present the same experimental fingerprints (i.e., those of BP), unless electrons are promoted onto the levels of the vacancy by light at low temperature (to prevent their escape into polaron states). The BP in rutile can be excited by discrete energies to reach sites farther from the donor, resembling crudely a hydrogenic series of states. In anatase, both V_O and Ti_i are shallower than in rutile and are expected to be ionized at room temperature. The ionization energy of the remaining electrons happens to be near to that of the BP in rutile, so it seems likely that the "intrinsic defect-related" photoelectron peak, observed around 1 eV below the CB in both rutile and anatase, has actually different origin in different samples. Finally, we have shown that V_O is the dominant oxygen deficiency defect in weakly reduced intrinsic TiO_2, and Ti_i plays a major role only in strongly reduced intrinsic (especially anatase) samples or in case of *p*-type doping. We note that the latter fact is quite important from the view-point of band gap engineering in rutile with nitrogen (*p*-type) doping for visible-light photocatalysis but also for the possible exploitation of room-temperature ferromagnetism, which has been observed in intrinsically *p*-type oxygen rich anatase. The analysis provided here may help the interpretation of experiments in terms of Ti_i or V_O and contribute to the understanding of charge transport in bulk TiO_2 [75].

ACKNOWLEDGEMENTS

Fruitful discussions with C. Wöll and the support of the Supercomputer Center of Northern Germany (HLRN Grant No. hbc00011) is acknowledged.

[1] In ionic crystals with strong electron-phonon coupling (such as many II-VI semiconductors, alkali halides, oxides, etc.), a charge carrier is dressed in a cloud of virtual phonons and can be considered as a new composite particle, called a polaron. If the phonon cloud corresponds to a strong local relaxation of the lattice, the carrier is essentially trapped in a so-called "small polaron" state and transport can proceed only through thermally activated hopping.

[2] N.B.: we use, e.g., Ti(3+) as notation for the oxidation state, while Ti_i^{3+} denotes an interstitial Ti atom in the triply negative charged state.

[3] P. Deák, B. Aradi, and T. Frauenheim, Phys. Rev. B **83**, 155207 (2011).

[4] M. Setvin, C. Franchini, X. Hao, M. Schmid, A. Janotti, M. Kaltak, C. G. Van de Walle, G. Kresse, and U. Diebold, Phys. Rev. Lett. **113**, 086402 (2014).

[5] T. Sarkar, K. Gopinadhan, Zh. Jun, S. Saha, J. M. D. Coey, Y. P. Feng, A. Ariando, and T. Venkatesan (unpublished).

[6] P. Deák, J. Kullgren, and T. Frauenheim, Phys. Status Solidi RRL **8**, 583 (2014).

[7] S. K. Wallace and K.P. McKenna, J. Phys. Chem. C **119**, 1913 (2015).

[8] S. Wendt, P. T. Sprunger, E. Lira, G. K. H. Madsen, Z. S. Li, J. O. Hansen, J. Matthiesen, A. Blekinge-Rasmussen, E. Laegsgaard, B. Hammer, and F. Besenbacher, Science **320**, 1755 (2008).

[9] C. M. Yim, C. L. Pang, and G. Thornton, Phys. Rev. Lett. **104**, 036806 (2010).

[10] M. Aono and R. R. Hasiguti, Phys. Rev. B **48**, 12406 (1993).

[11] C. L. Pang, R. Lindsay, and G. Thornton, Chem. Soc. Rev. **37**, 2328 (2008).

[12] P. Deák, B. Aradi, and T. Frauenheim, Phys. Rev. B **86**, 195206 (2012).

[13] S. Lany and A. Zunger, Phys. Rev. B **80**, 085202 (2009).

[14] P. Deák, B. Aradi, T. Frauenheim, E.Janzén, and A. Gali, Phys. Rev. B **81**, 153203 (2010).

[15] HF exchange gives a total energy, which is a concave, while local/semi-local DFT is a convex function of the fractional occupation numbers. Proper mixing may lead to linear behavior, with the correlation- and the self-interaction error cancelling each other.

[16] X. Zheng, A. J. Cohen, P. Mori-Sanchez, X. Hu, and W. Yang, Phys. Rev. Lett. **107**, 026403 (2011).

[17] S. J. Clark and J. Robertson, Phys. Rev. B **82**, 085208 (2010); K. Xiong, J. Robertson, M. C. Gibson, and S. J. Clark, Appl. Phys. Lett. **87**, 183505 (2005).

[18] J. Heyd, G. E. Scuseria, and M. Ernzerhof, J. Chem. Phys. **118**, 8207 (2003).

[19] J. A. V. Krukau, O. A. Vydrov, A. F. Izmaylov, and G. E. Scuseria, J. Chem. Phys. **125**, 224106 (2006).

[20] M. Marsman, J. Paier, A. Stroppa and G. Kresse, J. Phys. Condens. Matter **20**, 064201 (2008).

[21] J. P. Perdew, M. Ernzerhof, and K. Burke, J. Chem. Phys. **105**, 9982 (1996).

[22] P. Deák, B. Aradi, and T. Frauenheim, J. Phys. Chem. C **115**, 3443 (2011).

[23] A. D. J. Becke, J. Chem. Phys. **98**, 5648 (1993); C. Lee, W. Yang, and R. G. Parr, Phys. Rev. B **37**, 785 (1988).

[24] C. Di Valentin and A. Selloni, J. Phys. Chem. Lett. **2**, 2223 (2011).

[25] A. Janotti, J. B. Varley, P. Rinke, N. Umezawa, G. Kresse, and C. G. Van de Walle, Phys. Rev. B **81**, 085212 (2010).

[26] T. Yamamoto and T. Ohno, Phys. Chem. Chem. Phys. **14**, 589 (2012).

[27] T. S. Bjørheim, A. Kuwabara, and T. Norby, J. Phys. Chem. C **117**, 5919 (2013).

[28] B. J. Morgan and G. W. Watson, Phys. Rev. B **80**, 233102 (2009).

[29] B. J. Morgan and G. W. Watson, J. Phys. Chem. C **114**, 2321 (2010).

[30] G. Mattioli, P. Alippi, F. Filippone, R. Caminiti, and A. Amore Bonapasta, J. Phys. Chem. C **114**, 21694 (2010).

[31] J. Stausholm-Møller, H. H. Kistoffersen, B. Hinnemann, G. K. H. Madsen, and B. Hammer, J. Chem. Phys. **133**, 144708 (2010).

[32] E. Finazzi, C. Di Valentin, and G. Pacchioni, J. Phys. Chem. C **113**, 3382 (2009).

[33] H.-Y. Lee, S. J. Clark, and J. Robertson, Phys. Rev. B **86**, 075209 (2012).

[34] G. Kresse and J. Hafner, Phys. Rev. B **49**, 14251 (1994); G. Kresse and J. Furthmüller, *ibid.* **54**, 11169 (1996); G. Kresse and D. Joubert, *ibid.* **59**, 1758 (1999).

[35] J. Pascual, J. Camassel, and H. Mathieu, Phys. Rev. B **18**, 5606 (1978).

[36] H. Tang, F. Lévy, H. Berger, and P. E. Schmid, Phys. Rev. B **52**, 7771 (1995).

[37] Y. Tezuka, S. Shin, T. Ishii, T. Ejima, S. Suzuki, and S. Sato, J. Phys. Soc. Jpn. **63**, 347(1994).

[38] S. Rangan, S. Katalinic, R. Thorpe, R. A. Bartynski, J. Rochford, and E. Galoppini, J. Phys. Chem. C **114**, 1139 (2010).

[39] W. Kang and M. S. Hybertsen, Phys. Rev. B **82**, 085203 (2010).

[40] L. Chiodo, J. M. García-Lastra, A. Iacomino, S. Ossicini, J. Zhao, H. Petek, and A. Rubio, Phys. Rev. B **82**, 045207 (2010).

[41] M. Landmann, E. Rauls, and W. G. Schmidt, J. Phys.: Condens. Matter **24**, 195503 (2012).

[42] In the Brillouin-zone of orthogonal lattices, this is the point where a tight binding band of the interacting defects is closest to the level of an isolated defect.

[43] H. J. Monkhorst and J. K. Pack, Phys. Rev. B **13**, 5188 (1976).

[44] S. Lany and A. Zunger, Phys. Rev. B **78**, 235104 (2008).

[45] S. Lany and A. Zunger, Phys. Rev. B **81**, 113201 (2010).

[46] H.-P. Komsa, T. T. Rantala, and A. Pasquarello, Phys. Rev. B **86**, 045112 (2012).

[47] P. Deák, Phys. Status Solidi B **217**, 9 (2000).

[48] B. Lee, C.-K. Lee, C. S. Hwang, and S. Han, Curr. Appl. Phys. **11**, S293 (2011).

[49] P. Kofstad, *Non-Stoichiometry, Diffusion, and Electrical Conductivity in Binary Metal Oxides* (Wiley, New York, 1972).

[50] T. Bak, J. Nowotny, and M. K. Nowotny, J. Phys. Chem. B **110**, 21560 (2006).

[51] S. Yang, A. T. Brant, N. C. Giles, and L. E. Halliburton, Phys. Rev. B **87**, 125201 (2013).

[52] D. C. Cronemeyer, Phys. Rev. **113**, 1222 (1959).

[53] W.-T. Kim, C.-D. Kim, and Q. W. Choi, Phys. Rev. B **30**, 3625 (1984).

[54] A. K. Gosh, F. G. Wakim, and R. R. Addiss Jr., Phys. Rev. **184**, 979 (1969).

[55] S. Yang, L. E. Halliburton, A. Mannivanan, P. H. Bunton, D. B. Baker, M. Klemm, S. Horn, and A. Fujishima, Appl. Phys. Lett. **94**, 162114 (2009).

[56] F. D. Brandão, M. V. B. Pinheiro, G. M. Ribeiro, G. Medeiros-Ribeiro, and K. Krambock, Phys. Rev. B **80**, 235204 (2009).

[57] V. E. Henrich and R. L. Kurtz, Phys. Rev. B **23**, 6280 (1981).

[58] R. Sanjines, H. Tang, H. Berger, F. Gozzo, G. Margaritondo, and F. Levy, J. Appl. Phys. **75**, 2945 (1994).

[59] A. G. Thomas, W. R. Flavell, A. K. Mallick, A. R. Kumarasinghe, D. Tsoutsou, N. Khan, C. Chatwin, S. Rayner, G. C. Smith, R. L. Stockbauer, S. Warren, T. K. Johal, S. Patel, D. Holland, A. Taleb, and F. Wiame, Phys. Rev. B **75**, 035105 (2007).

[60] H. Sezen, M. Buchholz, A. Nefedov, C. Natzeck, S. Heissler, C. Di Valentin, and C. Wöll, Sci. Rep. **4**, 3808 (2014).
[61] H. Najafov, S. Tokita, S. Osshio, A. Kati, and H. Saitoh, Japn. J. Appl. Phys. **44**, 245 (2005).
[62] H. Sezen, H. Shang, F. Bebensee, C. Yang, M. Buchholz, A. Nefedov, S. Heissler, C. Carbogno, M. Scheffler, P. Rinke, and C. Wöll, Nat. Commun. **6**, 6901 (2015).
[63] S. Moser, L. Moreschini, J. Jaćimović, O. S. Barišić, L. H. Berger, A. Magrez, Y. J. Chang, K. S. Kim, A. Bostwick, E. Rotenberg, L. Forró, and M. Grioni, Phys. Rev. Lett. **110**, 196403 (2013).
[64] R. Asahi, T. Morikawa, T. Ohwaki, K. Aoki, and Y. Taga, Science, **293**, 269 (2001).
[65] C. Di Valentin, G. Pacchioni, A. Selloni, S. Livraghy, and E. Giamello, J. Phys. Chem. B **109**, 11414 (2005).
[66] J. B. Varley, A. Janotti, and C. G. Van de Walle, Adv. Mater. **23**, 2343 (2011).
[67] C. N. Druckworth, A. W. Brinkman, and J. Woods, Phys. Status Solidi A **75**, K99 (1983).
[68] B. Santara, P. K. Giri, K. Imakita, and M. Fujii, J. Phys. Chem. C **117**, 23402 (2013).
[69] L. Forro, O. Chauvet, D. Emin, and L. Zuppiroli, J. Appl. Phys. **75**, 633 (1994).
[70] Note that the first and second vertical ionization energies of the EMT states of Ti_i are computed to be equal (cf. Table I), and the first adiabatic charge transition in Fig. 5 is $(2+/0)$. The accuracy of the supercell method is quite limited, in case of shallow EMT states.
[71] T. Shibuya, K. Yasuoka, S. Mirbt, and B. Sanyal, J. Phys.: Condens. Matter. **24**, 435504 (2012).
[72] M. J. Jackman, P. Deák, K. L. Syres, J. Adell, B. Thiagarajan, A. Levy and A. G. Thomas, arXiv:1406.3385 [cond-mat.mtrl-sci]
[73] S. Wang, L. Pan, J.-J. Song, W. Mi, J.-J. Zou, L. Wang, and X. Zhang, J. Am. Chem. Soc. **137**, 2975 (2015).
[74] A. Rusydi, S. Dhar, A. Roy Barman, Ariando, D.-C. Qi, M. Motapothula, J. B. Yi, I. Santoso, Y. P. Feng, K. Yang, Y. Dai, N. L. Yakovlev, J. Ding, A. T. S. Wee, G. Neuber, M. B. H. Breese, M. Ruebhausen, H. Hilgenkamp, and T. Venkatesan, Phil. Trans. R. Soc. London, Ser. A **370**, 4927 (2012).
[75] M. K. Nowotny, T. Bak, and J. Nowotny, J. Phys. Chem. B **110**, 16270 (2006).